Journal of Applied Electrochemistry **29**: 1285–1289, 1999.

Fabrication and evaluation of 1 Ah silver/metal hydride cells

S. RODRIGUES[1], N. MUNICHANDRAIAH[2]* and A.K. SHUKLA[1]
[1]*Solid State and Structural Chemistry Unit;*
[2]*Department of Inorganic and Physical Chemistry, Indian Institute of Science, Bangalore 560 012, India*
*(*author for correspondence, e-mail: muni@ipc.iisc.ernet.in)*

Received 18 January 1999; accepted in revised form 31 March 1999

Key words: AB_2 alloy, cell discharge capacity, hydrogen storage alloy, impedance, silver/metal–hydride cell

Abstract

Silver/metal hydride (Ag/MH) cells of about 1 Ah capacity have been fabricated and their discharge characteristics at different rates of discharge, faradaic efficiency, cycle life and a.c. impedance have been evaluated. These cells comprise metal–hydride electrodes prepared by employing ~60 μm powder of an AB_2-Laves phase alloy of nominal composition $Zr_{0.5}Ti_{0.5}V_{0.6}Cr_{0.2}Ni_{1.2}$ with PTFE binder on a nickel-mesh substrate as the negative plates and commercial-grade silver electrodes as the positive plates. The cells are positive limited and exhibit two distinct voltage plateaus characteristic of two-step reduction of AgO to Ag during their low rates of discharge between $C/20$ and $C/10$. This feature is, however, absent when the cells are discharged at $C/5$ rate. On charging the cells to 100% of their capacity, the faradaic efficiency is found to be 100%. The impedance of the Ag/MH cell is essentially due to the impedance of the silver electrodes, since MH electrodes offer negligible impedance. The cells may be subjected to a large number of charge–discharge cycles with little deterioration.

1. Introduction

In recent years, metal hydrides have been found to be viable replacements for toxic cadmium electrodes of nickel/cadmium (Ni/Cd) cells [1, 2]. Nickel/metal hydride (Ni/MH) batteries also provide relatively high energy density and longer cycle life. Another system, that employs metal hydride electrodes, is the silver/metal hydride (Ag/MH) battery. The Ag/MH cell combines the high energy density of the silver electrodes with the long cycle life of the metal hydride electrodes and, thus, potential improvement in performance over Ni/MH and silver/zinc (Ag/Zn) cells. The half-cell reactions during charge–discharge of the Ag/MH cells are as follows.
At the negative electrode:

$$2\,MH + 2\,OH^- \underset{\text{charge}}{\overset{\text{discharge}}{\rightleftharpoons}} 2\,M + 2\,H_2O + 2\,e^- \quad (1)$$
$$(E^\circ = -0.93\,V \text{ vs MMO})$$

and at the positive electrode:

$$2\,AgO + H_2O + 2\,e^- \underset{\text{charge}}{\overset{\text{discharge}}{\rightleftharpoons}} Ag_2O + 2\,OH^- \quad (2)$$
$$(E^\circ = 0.51\,V \text{ vs MMO})$$

On further discharge, Ag_2O is reduced to Ag following the reaction:

$$Ag_2O + H_2O + 2\,e^- \underset{\text{charge}}{\overset{\text{discharge}}{\rightleftharpoons}} 2\,Ag + 2\,OH^- \quad (3)$$
$$(E^\circ = 0.29\,V \text{ vs MMO})$$

The overall cell reaction, thus, is given as

$$2\,MH + 2\,AgO \underset{\text{charge}}{\overset{\text{discharge}}{\rightleftharpoons}} 2\,M + Ag_2O + H_2O \quad (4)$$
$$(E^\circ_{\text{cell}} = 1.44\,V)$$

The cell has a nominal voltage of about 1.4 V, which is marginally higher than the cell voltage of 1.35 V for the Ni/MH system. In the literature, the studies on the Ag/MH cells are rather scanty. Eagle Picher were the first to report the development of Ag/MH cells for aerospace and military applications [3–5]. Some preliminary studies on bipolar Ag/MH cells have also been reported [6]. But, these studies are limited to determining the capacity of the Ag/MH cells and their ability towards charge retention.

In this communication, we report detailed investigations on fabrication of Ag/MH cells using AB_2 metal hydride electrodes and commercial-grade silver-positive plates along with their discharge characteristics, cycle life and a.c. impedance behaviour at various state-of-charge values. The study suggests that primarily the impedance of the positive Ag-electrodes limits the performance of these Ag/MH cells.

2. Experimental details

An ingot (~500 g) of $Zr_{0.5}$ $Ti_{0.5}$ $V_{0.6}$ $Cr_{0.2}$ $Ni_{1.2}$ alloy was prepared from the spongey constituent elements by repeated arc melting under an argon atmosphere in the range 10^{-3}–10^{-4} Pa in a water-cooled copper crucible. The alloy was pulverized mechanically and was passed through graded sieves to obtain alloy particles in the range 50–73 μm (average particle-size 60 μm).

Roll-compacted metal hydride electrodes were prepared following the procedure reported elsewhere [7]. In brief, the alloy powder (85 wt%), graphite (10 wt%) and polytetrafluoroethylene (PTFE) GP2-Fluon suspension (5 wt%) were mixed intimately, and the resulting paste was spread as a thin layer onto a degreased nickel mesh (4 cm × 3 cm) followed by compaction at a pressure of 3000 kg cm^{-2} for 5 min and heat treatment in hydrogen atmosphere at 350 °C for 30 min. Positive limited 1.4 V/1 Ah Ag/MH secondary cells were assembled using commercial Ag electrodes, which were stacked alternatively with the metal hydride electrodes. The electrodes were separated by a polypropylene cloth and were housed in polypropylene containers. The cells were filled with 6 M KOH electrolyte and had the provision to insert a microtipped Hg/HgO, KOH (6 M) reference electrode (MMO) for measuring the individual electrode potentials. All the experiments were carried out at ambient temperature (~30 °C) but for the a.c. impedance measurements, which were carried out in an air conditioned room maintained at 20 ± 1 °C. The batteries were subjected to a few initial charge–discharge cycles at $C/20$ rate. The electrodes were formed during these low rate charge–discharge cycles. Thereafter, a charge–discharge schedule at the $C/10$ rate was adopted. The electrical circuit for charge–discharge cycles consisted of a regulated d.c. power source, a high resistance and an ammeter in series. The cell voltage and electrode potentials were measured using a digital multimeter with a high input impedance. An impedance analyser (EG&G PARC model 6310) was employed for the a.c. measurements of the cells. The cell was excited with an a.c. signal amplitude of 5 mV in the frequency range from 100 kHz to 5 mHz. The state-of-charge (SOC) at a cut-off voltage of 1 V was taken as zero. The cell was fully charged at the $C/10$ rate and allowed to stand on open circuit for 2 h before the a.c. impedance measurements were carried out. The cell was allowed to reach equilibrium conditions under open circuit for 2 h prior to each impedance measurement.

3. Results and discussion

The ingot, as well as the powdered samples of $Zr_{0.5}$ $Ti_{0.5}$ $V_{0.6}$ $Cr_{0.2}$ $Ni_{1.2}$ alloy, were subjected to powder XRD and SEM studies [7]. The data suggested that the alloy was homogeneous in composition and its structure conforms to AB_2-Laves phases. The electrochemical reactions corresponding to individual electrodes of Ag/MH cells are given in Equations 1–3. In the charged state, the positive electrode constitutes essentially AgO, the discharge of which proceeds in two steps [8]. In the first step (Equation 2), Ag_2O is formed, which subsequently undergoes reduction to Ag in the second step (Equation 3). Since the reversible potentials of the two steps are distinctly different, the potential of the Ag electrode varies in two separate plateau-regions during charge/discharge of the Ag/MH cell.

The 1.4 V/1 Ah Ag/MH cells were subjected to charge–discharge cycles at several rates and typical data of cell voltage together with potentials of the individual electrodes at $C/20$ and $C/5$ rates are shown in Figures 1 and 2, respectively. The cells were discharged to a cut-off voltage of 1 V, where the corresponding silver and metal hydride electrode potentials were 0.15 V and −0.85 V vs MMO. At low rates of discharge between $C/20$ and $C/10$, two plateaus for the cell voltage were observed essentially due to the variation in the Ag electrode potential. During charging (Figure 1), the nominal cell-voltage values corresponding to the two plateaus were 1.48 V and 1.17 V and the respective values of Ag electrode potential were 0.56 V and 0.27 V vs MMO. On the other hand, the potential of the MH was nearly invariant at a value of −0.91 V vs MMO. On comparing the cell voltage during its charge and discharge, the overvoltages for the two plateaus of the cell were about 0.1 V (high-voltage plateau) and 0.08 V (low-voltage plateau). These values corresponded to the overvoltages of the Ag electrode during its charge–discharge processes. It may be noted from Figures 1 and 2 that, the cell capacity was limited by the positive silver plates. The cell delivered an average capacity of 1.1 Ah at the $C/10$ rate (discharge current 0.1 A).

The faradaic efficiency of the cell obtained at the $C/10$ rate as a function of the charge input is shown in Figure 3. The faradaic efficiency close to 100% was achieved when the cell was charged to 80% of its nominal capacity. At charge inputs >100%, the cell delivered a capacity of 1 Ah. The faradaic efficiency, however, decreased from 92% to 60% with an increase of charge input from 100% to 160% of its nominal capacity. These data suggest that the maximum cell capacity may be obtained by charging the cell to 100% of its nominal capacity; the overcharging of the cell seemingly does not influence its discharge capacity. Overcharging, by contrast, may affect the cell performance due to the evolution of oxygen and hydrogen gases at the Ag and MH electrodes, respectively.

The Ag/MH cells were subjected to charge–discharge cycles at different rates. The cell capacity decreased with an increase in charge–discharge rate as shown in Figure 4. The decrease in cell capacity on increasing the discharge current may be attributed to the discharge behaviour of the silver electrodes, as seen from Figures 1 and 2. During charging of the cell at the $C/20$ rate, the two potential plateau regions of the Ag electrode are clearly separated atleast by about 0.3 V (Figure 1(a)).

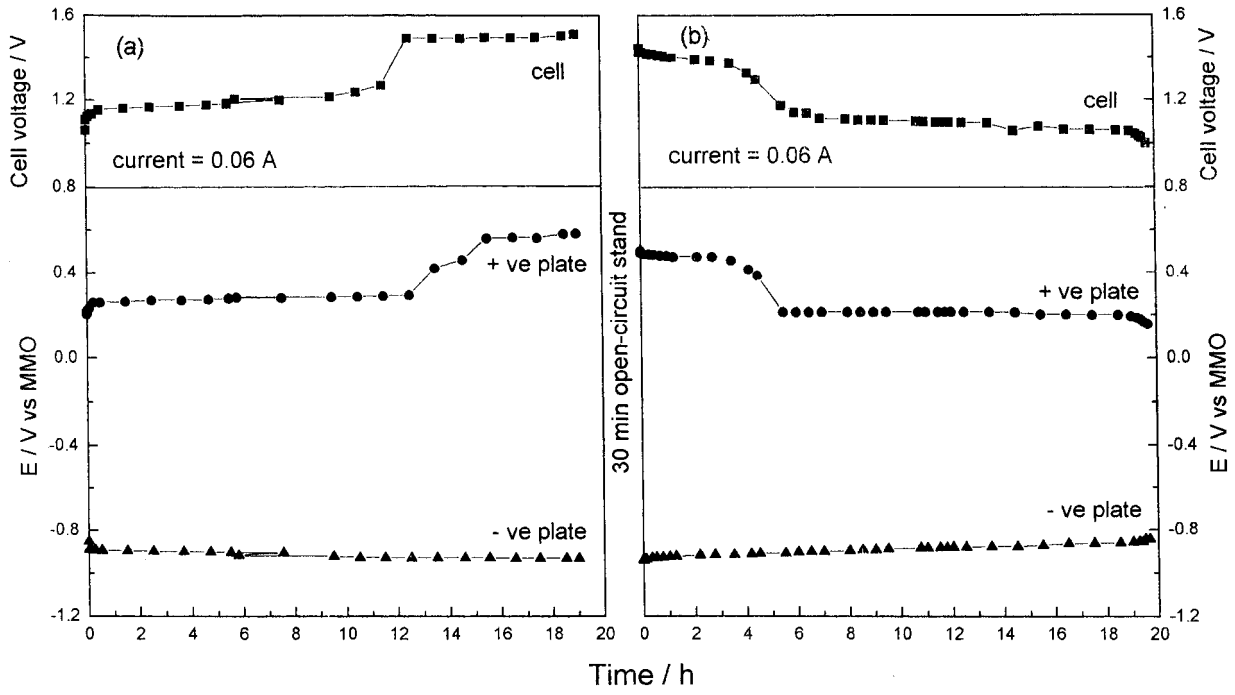

Fig. 1. Variation of Ag/MH cell voltage and individual electrode potentials at $C/20$ rate during (a) charge and (b) discharge.

Similarly, during discharge at the $C/20$ rate, the two plateaus are well separated by about the same magnitude (Figure 1(b)). During $C/5$ rate charging (Figure 2(a)), however, the lower-potential plateau of the Ag electrode is higher due to its higher overpotentials than at the $C/20$ rate charging (Figure 1(a)). Since the potential regions are closely located during charging at $C/5$ rate, the oxidation of Ag to AgO (Equations 3 and 4) may not be quantitatively complete before oxygen evolution reaction commences. On initiation of discharge at $C/5$ rate (Figure 2(b)), the Ag electrode potential falls rapidly to the second plateau due to a high overvoltage, yielding most of the discharge capacity of the cell at about 1.1 V. The high rates of discharge, therefore, are not favourable. Besides, the following aspects of Ag electrodes are also not conducive for high discharge rates. Silver oxide has a pronounced tendency to form colloids in alkaline electrolyte, which are transported to the negative plate due to cataphoresis [8]. This factor decreases the capacity of the cell and causes internal short circuiting. It is known that the electrical resistance of Ag_2O is considerably higher than AgO. As the oxidation of silver

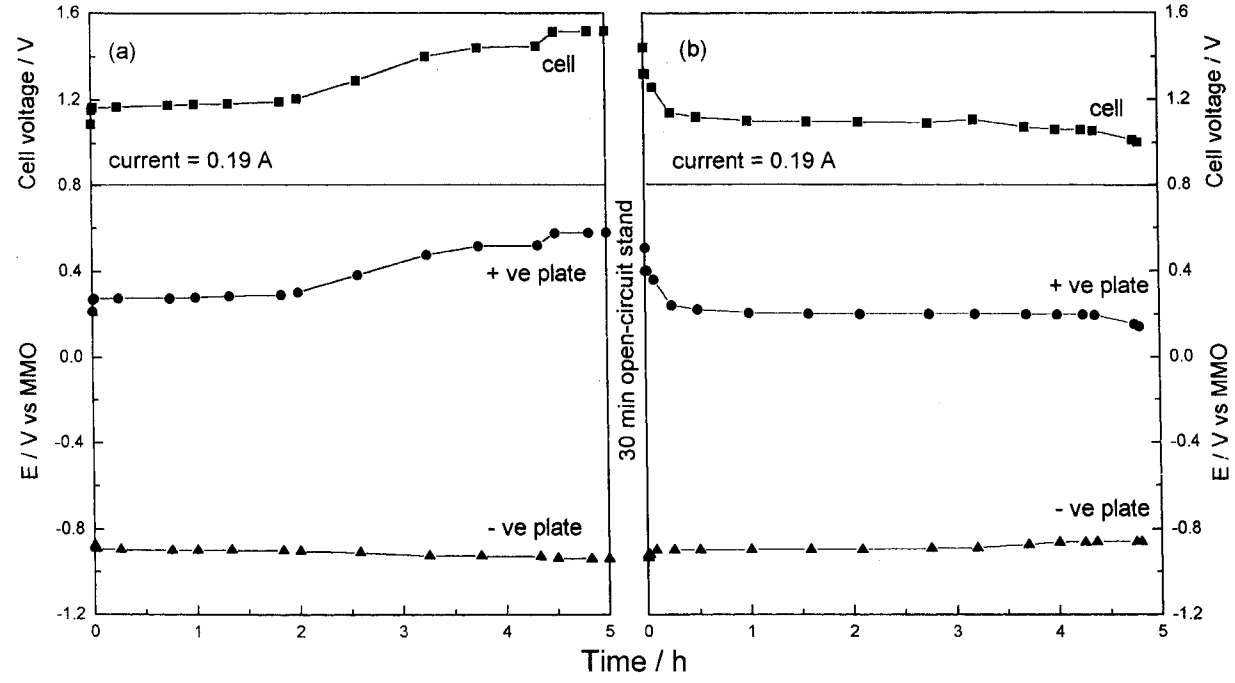

Fig. 2. Variation of Ag/MH cell voltage and individual electrode potentials at $C/5$ rate during (a) charge and (b) discharge.

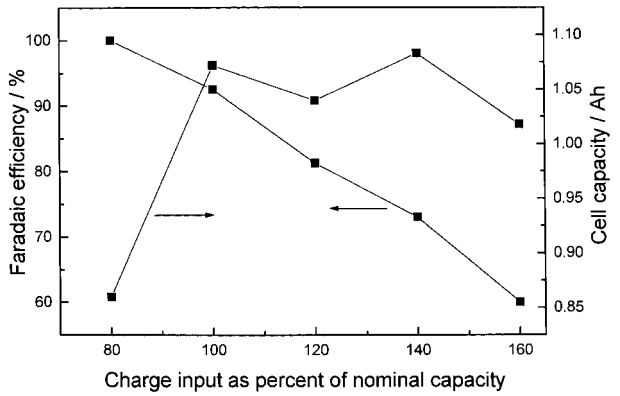

Fig. 3. Faradaic efficiency (%) and capacity (Ah) of the Ag/MH cell as a function of charge input.

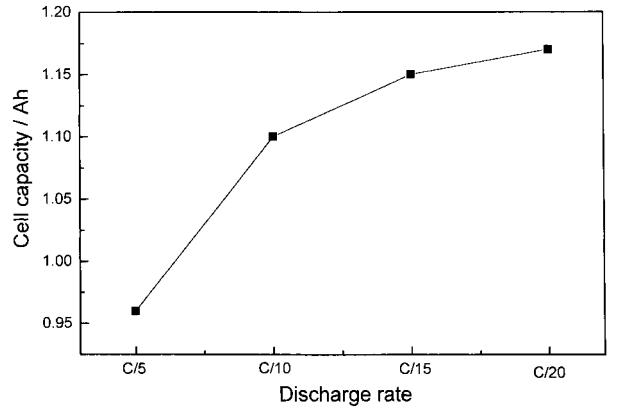

Fig. 4. Capacity (Ah) of the Ag/MH cell as a function of its discharge rate.

proceeds during initial charging, a film of Ag_2O is formed on the surface of the electrode. During high rates of charging, Ag_2O film builds up and increases the resistance at the electrode/electrolyte interface. During the second plateau of cell charging, Ag_2O is oxidized to AgO and the resistance of the surface film decreases [9]. Since high rates of charge–discharge do not favour the performance of the Ag/MH cell, $C/10$ rate was chosen for obtaining the cycle-life data. The capacity of the cell over about 40 cycles is shown in Figure 5. The first few cycles gave low cell capacity followed by a nearly constant capacity of about 1 Ah.

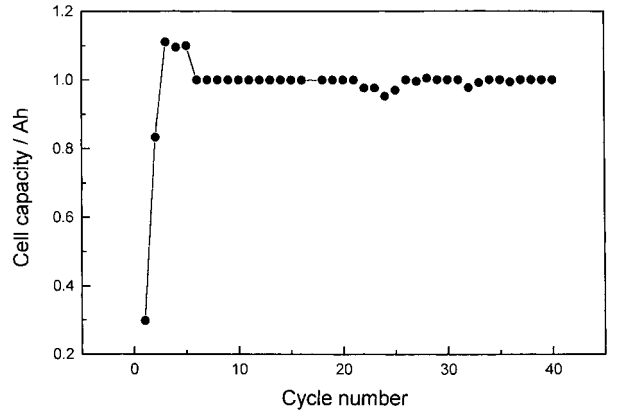

Fig. 5. Cycle-life data of the Ag/MH cell at $C/10$ rate.

The impedance spectra for the Ag/MH cell at SOC ~1 and for the individual electrodes are shown in Figure 6. All three sets of data points take the shape of semicircles in the Nyquist plots suggesting a parallel combination of resistances and capacitances in the corresponding equivalent circuits. An estimation of the diameter of the semicircle provides the charge-transfer resistance (R_{ct}) of the electrochemical reaction. A comparison of the impedance data in Figure 6 suggests that the MH electrodes have negligibly smaller impedance in relation to Ag electrodes. Also, the impedance of the Ag/MH cell is similar to Ag electrodes. These

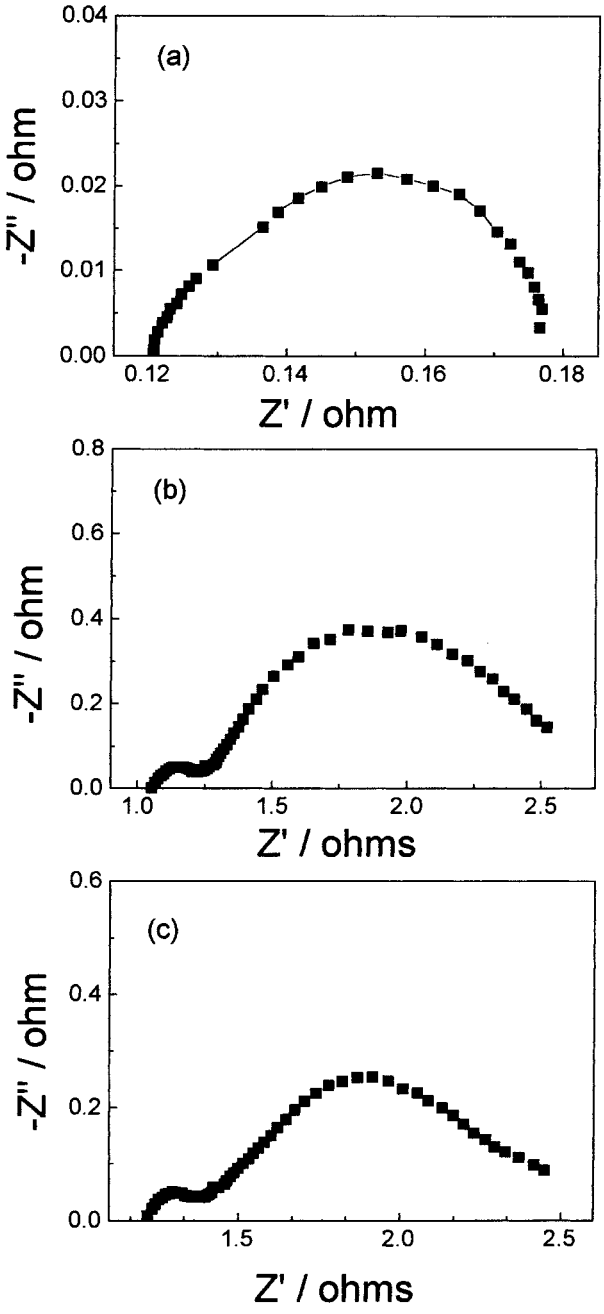

Fig. 6. A.c. impedance spectrum of (a) MH-electrode, (b) Ag-electrode and (c) the Ag/MH cell at SOC ~1.

observations also suggest that the performance of the Ag/MH cell is mainly governed by the kinetics of the Ag electrode reactions.

Since the Ag electrode behaviour is different in the two voltage plateaus, it is of interest to examine the nature of the impedance data of Ag/MH cells in these two regions as well as at the transient region between the two plateau-regions (Figure 7). The high-frequency intercept of the impedance of the cell at a voltage of 1.42 V (Figure 7(a)) is 1.2 Ω whereas at 1.08 V the intercept is 0.3 Ω. Since the high-frequency intercept provides ohmic resistance of the cell, which includes the resistance of the electrolyte, the current collectors, electrode materials etc., a higher value of 1.2 Ω at 1.42 V accounts for the presence of AgO phase, the resistance of which is higher than Ag. The lower ohmic resistance of 0.45 Ω at 1.08 V is due to more conducting Ag phase in the positive electrodes. At a cell voltage of 1.2 V, prior to change over of the cell from 1.4 V plateau to 1.1 V plateau, the ohmic resistance is as high as 2.35 Ω. This is because the electrode essentially consists of Ag_2O phase. Since the diameter (or low-frequency intercept) is a measure of R_{ct} of the electrochemical reactions occurring at the Ag electrodes, a comparison of the three sets of data in Figure 7 reveals that R_{ct} value of about 70 Ω obtained from Figure 7(b) is considerably higher than R_{ct} value of $<2.5\,\Omega$ obtained from Figure 7(a) and (c). Accordingly, the reaction corresponding to AgO/Ag_2O couple is highly sluggish in relation to the Ag/Ag_2O couple.

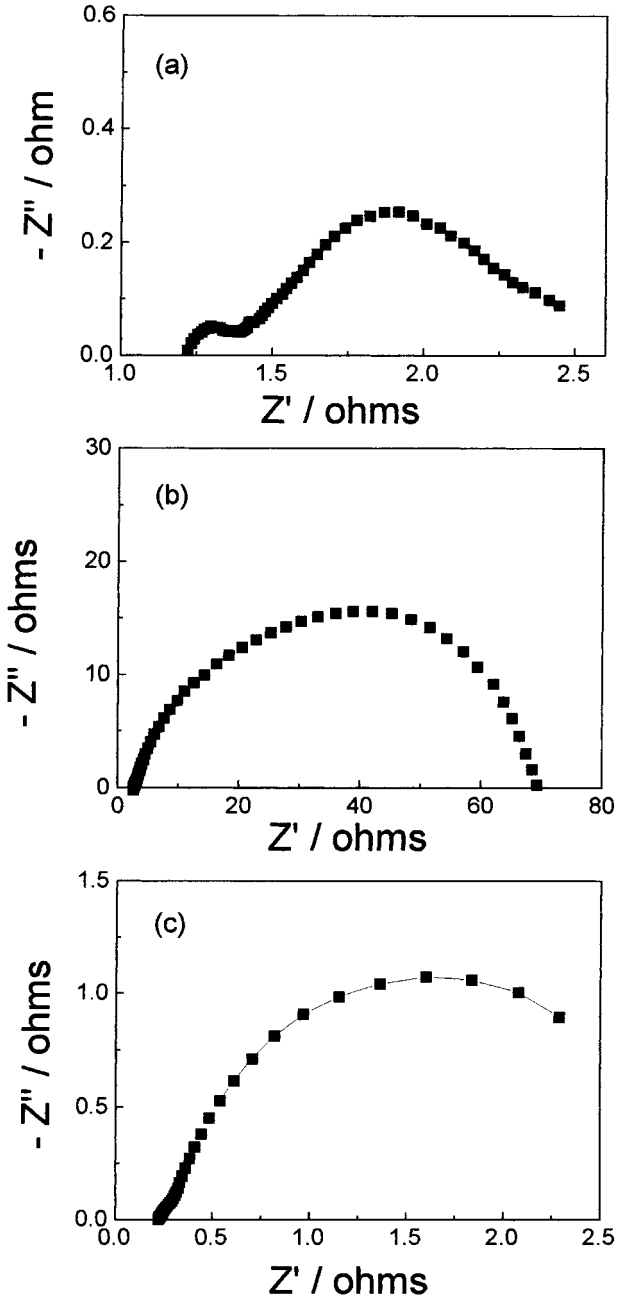

Fig. 7. A.c. impedance spectrum of the Ag/MH cell at the cell voltage of (a) 1.42, (b) 1.20 and (c) 1.09 V.

4. Conclusions

The AB_2-alloy of composition $Zr_{0.5}\,Ti_{0.5}\,V_{0.6}\,Cr_{0.2}\,Ni_{1.2}$ has been successfully employed for fabrication of metal hydride electrodes and assembly of Ag/MH cells of 1 Ah capacity. The cell performance is limited by the Ag electrodes and not the MH electrodes since the impedance of the latter is negligibly smaller than the Ag electrodes. A nominal discharge capacity of about 1 Ah has been obtained at the $C/10$ rate even when the cells are not overcharged. A constant cell capacity over forty charge–discharge cycles suggests that Ag/MH cells are suitable for commercial exploitation.

Acknowledgements

The technical support from the Indian Space Research Organization is gratefully acknowledged.

References

1. M.A. Fecenko, S. Venkatesan and S.R. Ovshinsky, D.A. Corrigan, and S. Srinivasan (Eds.), *Proc. Electrochem. Soc.* (The Electrochemical Society, Pennington, NJ), Vol. **92–5** (1992) pp. 141–167.
2. A. Anani, A. Visintin, K. Petrov, S. Srinivasan, J.J. Reilly, J.R. Johnson, R.B. Schwarz and P.B. Desch, *J. Power Sources* **47** (1994) 261.
3. D. Coates, C. Fox, and L. Miller, Proceedings of the 27th Intersociety Energy Conversion Engineering Conference, San Diego, CA, Vol. **2** (1992), p. 2.165.
4. T. Harvey and B. Hawkins, Proceedings of the 28th Intersociety Energy Conversion Engineering Conference, Atlanta, GA, Vol. **1** (1993), p. 1.681.
5. C.A. Vincent and B. Scrosati, 'Modern Batteries, An Introduction to Electrochemical Power Sources', 2nd edn, (Arnold, London, 1997), p. 197.
6. D.E. Reisner, R.F. Plivelich and M.G. Klein, Proceedings of the 30th Intersociety Energy Conversion Engineering Conference, Orlando, FA, Vol. **3** (1995), p. 235.
7. V. Ganesh Kumar, K.M. Shaju, N. Munichandraiah and A.K. Shukla, *J. Power Sources* **76** (1998) 106.
8. S.U. Falk and A.J. Salkind, 'Alkaline Storage Batteries', The Electrochemical Society, (J. Wiley & Sons, New York, 1969), p.156.
9. T.P. Dirkse and G.J. Werkema, *J. Electrochem. Soc.* **106** (1959) 88.